Clays and Clay Minerals, Vol. 31, No. 2, 97–108, 1983.

CRYSTAL STRUCTURE OF CRONSTEDTITE-$2H_2$

CHARLES A. GEIGER, DIANE L. HENRY, AND S. W. BAILEY
Department of Geology & Geophysics, University of Wisconsin–Madison
Madison, Wisconsin 53706

JOSEPH J. MAJ
Department of Chemistry, University of Wisconsin–Madison
Madison, Wisconsin 53706

Abstract—The crystal structure of a magnesian cronstedtite-$2H_2$ from Příbram, Czechoslovakia, was refined in space group $C1$ to a residual of 5.4% with 1832 independent reflections. Tetrahedral ordering between Fe^{3+} and Si is judged to be complete on the basis of electron density maps, the first confirmation of such ordering in a layer silicate. Octahedral cations are disordered on the M sites. Mean T–O bond lengths do not confirm the tetrahedral ordering, perhaps due to tetrahedral distortion in order to relieve the extreme corrugation of the sheet that would arise from ordering of such different size cations.

In the initial stages of refinement the structure of the crystal under study could not be described adequately on the basis of a single $2H_2$ polytype. The structure contains two kinds of $2H_2$ domains that appear shifted by $b/3$ relative to one another due to a mistake in the interlayer stacking sequence. This mistake of zero shift (the normal $2H_2$ polytype consists of alternating $-b/3$ and $+b/3$ shifts) affects only the tetrahedral sheets. It creates adjacent enantiomorphic domains of $2H_2$ packets such that domains with small Si tetrahedra sit above larger Fe^{3+}-rich tetrahedra and vice versa. This mechanism to relieve strain may indeed be the cause of the stacking mistakes. A third kind of domain contains regions in which the sense of tetrahedral rotation is reversed, giving rise to split basal oxygens on electron density maps. This multiple domain model best explains extra atomic positions observed on Fourier maps, lack of streaking of $k \neq 3n$ reflections, and possible nonintegral "satellitic" reflections observed on Weissenberg films.

Key Words—Amesite, Atomic positions, Cation ordering, Cronstedtite, Crystal structure, Iron, Serpentine.

INTRODUCTION

Cronstedtite is a trioctahedral 1:1 layer silicate with the ideal end member composition of $(Fe^{2+}{}_2Fe^{3+})(SiFe^{3+})O_5(OH)_4$. It typically occurs in low-temperature hydrothermal veins associated with siderite, pyrite, sphalerite, and quartz (Frondel, 1962). Cronstedtite also has been reported in carbonaceous chondrites (Müller *et al.*, 1979; Barber, 1981). Gole (1980) reported a possible occurrence of cronstedtite in an assemblage of low-temperature retrograde minerals found in a metamorphosed Australian iron formation of Archean age.

The various polytypes of cronstedtite, eight of which have been described in the literature, are formed by stacking the 1:1 serpentine layers in different manners, as described by Bailey (1969). Cronstedtite is a very iron-rich layer silicate, even more so than greenalite [approximately $Fe_3Si_2O_5(OH)_4$], in that it has ferric iron in tetrahedral coordination in addition to the iron in octahedral coordination. The presence of tetrahedrally coordinated ferric iron has long been recognized in some layer silicates. Various synthetic phases, such as the iron mica of composition $KFe^{2+}{}_3(Si_3Fe^{3+})O_{10}(OH)_2$ described by Donnay *et al.* (1964), rare phlogopites of composition $(K_{0.9}Mn_{0.1})Mg_3[Si_3(Fe^{3+},Mn)O_{10}(OH)_2$ (Steinfink, 1962), and the rare, brittle mica anandite (Pattiaratchi *et al.*, 1967) contain significant amounts of tetrahedrally coordinated Fe^{3+}. Inasmuch as Si and Fe^{3+} occur in a favorable tetrahedral ratio ideally near 1:1 and have radically different effective ionic radii in tetrahedral coordination, 0.26 Å and 0.49 Å (high spin), respectively (Shannon, 1976), the possibility of tetrahedral ordering should be investigated in cronstedtite.

In the $2H_2$ polytype of Bailey (1969) there are alternating interlayer shifts of $-b/3$ and $+b/3$ and alternating occupation of the I and II sets of octahedral positions in successive 1:1 layers. The $2H_2$ polytype of cronstedtite is essentially isostructural with amesite-$2H_2$, another 1:1 layer silicate which has an ideal composition of $(Mg_2Al)(SiAl)O_5(OH)_4$. Two structural analyses of amesite-$2H_2$ have indicated tetrahedral ordering of Al and Si (Hall and Bailey, 1979; Anderson and Bailey, 1981). The $2H_2$ polytypes of both cronstedtite and amesite are ideally hexagonal and of space group $P6_3$, but it will be shown that cation ordering and/or minor distortions in the structures have lowered their symmetries to subgroup $P1$. Hence, both structures are highly pseudosymmetric.

This paper reports an X-ray structural analysis and refinement of a $2H_2$ polytype of cronstedtite based on 1832 counter-collected reflections. Previous work has concentrated on other polytypes and has used a limited

Copyright © 1983, The Clay Minerals Society

https://doi.org/10.1346/CCMN.1983.0310203 Published online by Cambridge University Press

number of film-collected data (Steadman and Nuttall, 1963, 1964). These studies described partial refinements of 1*T*, 3*T*, $2H_1$, and $6R_2$ polytypes. No tetrahedral or octahedral ordering was found in the corresponding ideal space groups $P31m$, $P3_1$, $P6_3cm$, and R_3, respectively, of these cronstedtites. Steadman and Nuttall (1964) also described a two-layer cronstedtite of space group $P6_3$ from Wheal Maudlin, Cornwall. This is the $2H_2$ polytype, but no attempt was made at refinement. Steadman and Nuttall also noted that twinning and stacking mistakes are common in many cronstedtite polytypes, and that the 2*T* ($P31c$), $2M_2$ (Cc), and 1*M* (Cm) polytypes are present only as small twinned regions within other structures.

FILM-DATA REFINEMENT

As the first stage in the present study, two-dimensional *h*0*l* and 0*kl* Weissenberg film data were collected for a $2H_2$ polytype of cronstedtite from Příbram, Bohemia (Czechoslovakia), specimen 472:1 of the Colorado School of Mines collection kindly furnished by J. J. Finney. Only one $2H_2$ crystal could be found on the hand sample. This crystal had a distinctive ovoid- to barrel-shaped morphology with flat (001) surfaces and serrated edges. The same crystal was used for X-ray diffraction data collection and later for an electron probe study. The electron probe analysis yields the following structural formula

$$(Fe^{2+}_{1.640}Fe^{3+}_{0.486}Mg_{0.709}Mn^{2+}_{0.163}Ca_{0.002})(Si_{1.514}Fe^{3+}_{0.485}Al_{0.001})O_5(OH)_4.$$

It was assumed in this allocation that R^{3+} in tetrahedral coordination is balanced by an equal amount in octahedral coordination. This formula differs from the ideal in the smaller amount of Fe^{3+} plus the presence of substantial Mg. It should be called a magnesian cronstedtite.

All X-ray diffraction reflections from this crystal proved to be remarkably sharp for a layer silicate, with no streaking of $k \neq 3n$ reflections. In contrast, most crystals of other polytypes of cronstedtite examined in this study showed various amounts of streaking of the $k \neq 3n$ reflections, indicative of stacking mistakes. The lattice determined from the film data was dimensionally hexagonal, with no doubling of spots of the sort used to indicate twinning by Steadman and Nuttall for some of their crystals. Because of the jet black color of the crystal, optical observation of twinning by reflected or transmitted light, even with ultra-thin sections, proved impossible. Therefore, twinning of the type that exactly superimposes reflections could not be ruled out. A few extra spots observed on *hk*0 Weissenberg films were suggestive of non-Bragg satellites, except that they were not located symmetrically about their companion Bragg reflections. These were ignored in the structural refinement.

The intensities of reflections on multi-film Weissenberg photographs taken with MoKα were measured by visual comparison with standard intensity scales, then corrected for Lp and absorption factors. Initial least-squares refinement of the film data using the ORFLS program was performed in the ideal space group $P6_3$ because of lack of evidence indicating lower symmetry. The final mean T–O bond lengths and electron density maps indicated ordering of tetrahedral Fe^{3+} into site T(1) and of Si into site T(2). Ordering of the octahedral Fe^{2+}, Fe^{3+}, and Mg is not possible in $P6_3$ symmetry. The results of refinement to a residual R value of 12.6% were reported by Henry (1974) and of further refinement to R = 10.2% by Bailey (1975).

During this preliminary study it became apparent that ordering of Si and Fe^{3+} in tetrahedral sites can lead to an ambiguity in cursory identification of the $2H_1$ and $2H_2$ polytypes. Ideally, the $2H_2$ polytype of symmetry $P6_3$ is identified by the 2-layer periodicity evident in 0*kl* reflections with $k \neq 3n$ (orthohexagonal indexing) due to the presence of l = even and l = odd reflections, whereas in the $2H_1$ polytype of symmetry $P6_3cm$ the l = odd reflections of this type are systematically absent. Ordering of tetrahedral Fe^{3+} and Si would reduce the symmetry of the $2H_1$ polytype to $P6_3$, however, and the different scattering powers of Fe and Si would produce weak l = odd reflections. Calculations for the $2H_2$ polytype show that for reflections with orthohexagonal indices of type 02*l* all of the l = even intensities increase regularly and the l = odd intensities decrease regularly as the amount of Fe^{3+} in site T(1) is increased. For the $2H_1$ polytype the intensities of the l = even reflections are not affected by the ordering, but those for l = odd increase with the amount of Fe^{3+} in T(1), although always remaining less than those with l = even. A precautionary refinement of the experimental data treating the structure as an ordered $2H_1$ polytype showed that the crystal used in this study is truly a $2H_2$ polytype. This is evident also from the fact that the observed intensities of the 0*kl* reflections of type $k \neq 3n$ with l = odd are too strong relative to those with l = even for the ordered $2H_1$ model. It is still possible, however, that stacking mistakes leading to small regions of $2H_1$ can exist in the crystal.

COUNTER-DATA REFINEMENT

Refinement of the isostructural $2H_2$ polytype of amesite from two different localities by Hall and Bailey (1979) and Anderson and Bailey (1981) subsequent to the initial refinement of cronstedtite-$2H_2$ showed that amesite crystals are universally twinned on (001), have individual twin sectors that are anisotropic with 2V values near 18°, and are distorted slightly to triclinic unit-cell geometry. Cronstedtite-$2H_2$, with a different ordering pattern than amesite-$2H_2$, is not distorted geometrically, but its black color prevents optical confirmation of its symmetry or twinning. However, the combination of the amesite results, the observation that

https://doi.org/10.1346/CCMN.1983.0310203 Published online by Cambridge University Press

Table 1. Unit-cell parameters for cronstedtite-$2H_2$ from Příbram, Czechoslovakia.

Parameter	Henry (1974)[1]	This study[2]
a	5.473 Å	5.472(8) Å
b		9.467(19) Å
c	14.257 Å	14.241(39) Å
α		90.015(20)°
β	90.0°	90.042(18)°
γ		89.952(15)°
V		737.72(28) Å^3

[1] Determined from film using θ method of Weisz *et al.* (1948) and based on hexagonal symmetry, space group $P6_3$.

[2] Obtained from a least squares best fit of 15 medium to high-angle reflections collected on an automated $P2_1$ Syntex Diffractometer, and based on space group $C1$.

the cronstedtite mean T–O bonds lengths were not in good agreement with those expected for the bulk tetrahedral composition, and our inability to refine the cronstedtite film data below a residual of 10% led to further study.

The intensities of six reflections that should be equivalent in hexagonal symmetry were collected by a scintillation counter on a Syntex $P2_1$ diffractometer for the same crystal used in the film-data refinement. The observed 1.1 ratio between the largest and smallest intensities of these six reflections indicated an approximation to hexagonal symmetry. The large parent crystal then was cut into 20 smaller fragments, and the intensities of the same six reflections were collected for each fragment. Intensity ratios varying from 1.1 to 1.4 were recorded, suggesting that variable amounts of twinning are present in these fragments and that the normal and twin reflections exactly superimpose because of the metrically hexagonal unit cell (Table 1). From the intensities it was determined that the true symmetry is triclinic, although not far from monoclinic, and that the position of true Y^* could be determined by recognition that the $20l$ intensities are quite different than those of the related $13l$ and $1\bar{3}l$ reflections.

The crystal fragment showing the greatest deviation from hexagonal symmetry among the six monitored reflections was chosen for detailed study. For ease of comparison with amesite-$2H_2$, the structure was indexed using an orthohexagonal cell of space group $C1$. Unit-cell parameters (Table 1) were determined by least-squares refinement of 15 medium- to high-angle reflections on a Syntex $P2_1$ automated single crystal diffractometer. In contrast to amesite-$2H_2$, the unit cell of this cronstedtite-$2H_2$ is metrically orthorhombic with $\beta = 90°$.

The intensity data were collected in the 2θ:θ variable-scan mode using graphite-monochromatized MoKα radiation. A total of 1832 non-zero reflections were measured in four quadrants of the limiting sphere $0° < 2\theta < 60°$. Crystal and electronic stability were checked after every 50 reflections by monitoring a standard reflection. Reflections were considered observed if $I > 2\sigma(I)$, where I was calculated from $I = [S - (B_1 + B_2)/B_r]T_r$, with S being the scan count, B_1 and B_2 the background on each side of the peak, B_r the ratio of background time to scan time, and T_r the 2θ scan rate in degrees per minute. Values of $\sigma(I)$ were calculated from standard counting statistics. Integrated intensities were corrected for Lorentz and polarization effects, and for absorption by the empirical ψ scan technique.

Initial atomic coordinates from Bailey's (1969) ideal $2H_2$ model were used as the starting points for a full least-squares refinement of the reflection data in triclinic symmetry. The least-squares program ORFLS was used at the start of the refinement. Isotropic temperature factors of 0.6, 0.8, and 1.5 were assigned to the 28 T, M, and anion sites in the asymmetric unit. Using the results of the microprobe analysis, atomic scattering factors were calculated from the values reported in the *International Tables for X-Ray Crystallography*. It was assumed that all atoms were one-half ionized and that no cation ordering was present. The tetrahedral cation T(1) was kept stationary during refinement in order to fix the origin in this noncentrosymmetric structure. Late in the refinement the sense of the Z axis was determined by comparison of observed and calculated structure amplitudes.

Refinement was initiated using σ weights, and after one least-squares cycle R_w equaled 29.5%. After a number of cycles in which the scale factor and the atomic coordinates x, y, and z were varied, the R_w factor dropped to roughly 19%. After several more cycles in which the isotropic B values also were varied, R_w dropped to approximately 16%. At this point, because of the high values of R_w, it was obvious that the structure was not entirely correct. Electron density maps were made at various sections along the Z axis, therefore, using as input the atomic coordinates from the least-squares refinement with the smallest R factor. Anomalous extra peaks at the levels of the tetrahedral cations appeared at approximately $x = 0.0$, $y = 0.66$, $z = 0.04$, at $x = 0.0$, $y = 0.32$, $z = 0.55$, and at their symmetry-related equivalent positions. These peaks appeared to represent "twin" domains in which T(1) and T(11) were shifted by $b/3$; they were designated as atoms TwT(1) and TwT(11), respectively. Also, it was observed that the electron densities for the hydroxyl groups and the apical oxygens in the octahedral sheet were greater than those of the basal oxygens. Additional electron density and difference electron-density maps were constructed using F_o and F_c values that had been through only one least-squares cycle. This time extra electron-density peaks appeared also at $z = 0.0$ and $z = 0.50$, the level of the basal oxygens, and the observed electron densities at the T(1) and T(11) positions were too large based on the proposed ordering pattern. Consequently, two extra "twin" tetrahedral positions [TwT(2) and Tw-

https://doi.org/10.1346/CCMN.1983.0310203 Published online by Cambridge University Press

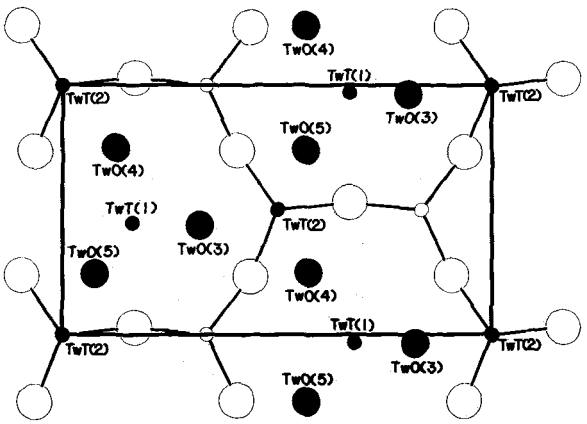


Figure 1. Projection onto (001) of the tetrahedral sheet in the first layer. Extra tetrahedral cations in out-of-step domains are designated by small solid circles and extra basal oxygens by larger solid circles.

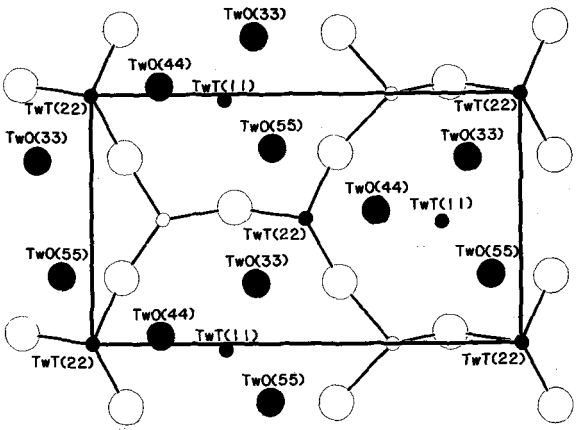


Figure 2. Projection onto (001) of the tetrahedral sheet in the second layer. Symbols as for Figure 1.

T(22)] were added to the structure as being coincident with T(1) and T(11) of the average structure. These two positions also are required to coordinate with the extra basal oxygens just noted above [designated TwO(3), TwO(4), TwO(5), and TwO(33), TwO(44), TwO(55)] and their tetrahedral cations [TwT(1) and TwT(11)]. All of these extra "twin" positions occur in a set of anomalous domains in which each tetrahedral sheet is out-of-step by $b/3$ relative to the rest of the structure. Octahedral sheet positions in the domains coincide with those of the normal $2H_2$ structure. Figures 1 and 2 illustrate the "twin" positions in each 1:1 layer.

Refinement was continued with the eight additional atomic positions, a total of 36 in the asymmetric unit. Multiplicities of the additional positions that did not overlap were set initially at 0.30 (Tw positions). All atomic positions that did coincide had multiplicities set equal to 1.3; these included all apical O, OH groups, M cations, T(1), and T(11). On the basis of electron density maps Fe^{3+} was ordered into T(1) and T(11) and into the two additional cation positions that did not overlap with the normal tetrahedral positions, i.e., TwT(I) and TwT(II). After several least-squares cycles the R factor dropped to ~11.5%. Other ordering patterns produced a small rise in the R factor. At this stage refinement was switched to unit weights, as this has been found to give better convergence for other layer silicate structures. Also, isotropic B values were allowed to vary from their ideal starting values. The R value dropped to 9%. Isotropic B values of the basal oxygens were larger than those of the apical oxygens, 2.2 to 2.6 vs. 1.1 to 1.4. Bond lengths, however, did *not* indicate ordering of ferric iron and silicon in the two independent tetrahedra. Mean T–O bond lengths for all tetrahedra were 1.68 Å to 1.70 Å. Moving basal oxygens to positions in accord with bond lengths calculated from ionic radii listed in Shannon (1976) had negative results, as the least-squares program moved the oxygens back to their former positions. Electron density maps constructed at that time continued to confirm ordering of tetrahedral Si and Fe^{3+}, but did show some electron smearing (i.e., positional disorder) for the basal oxygens.

At this point in the refinement many problems developed with the use of program ORFLS. First, the multiplicities of the various extra positions when varied did not remain equal; values ranged from 0.05 to 0.30. Hence, electron densities of these sites also became a function of the given multiplicity. It was crucial to determine the actual proportion of both sets of positions so that the ordering scheme could be verified. Second, isotropic thermal parameters varied greatly between similar atoms (basal oxygens) and were unrealistically large. Third, tetrahedral bond lengths were erratic and varied in no systematic manner in accord with the ordering pattern.

Upon the recommendation of Professor L. F. Dahl of the University of Wisconsin Chemistry Department, a second refinement was started with the recently written and more flexible least-squares program RAELS (by A. D. Rae, Department of Chemistry, University of New South Wales, Sydney, Australia). This refinement was based on F^2, instead of F as in ORFLS, which allows proper consideration of any twin or domainal models involving exact coincidence of reflections and also gives more emphasis to high-angle data. The same starting parameters were used for this refinement as were used with the ORFLS refinement. Sigma weights ($1/\sigma^2$) were assigned to all reflections during all stages of refinement. Also, slack constraints were constructed such that certain bond lengths remained nearly equal; i.e., all $T–O_b$ bonds were held in rigid groups for a given T site—T(1), T(22), etc. so that their lengths remained approximately equal during refinement. However, $T–O_a$ bond lengths were set independent of $T–O_b$ bond lengths, as these bond lengths commonly differ in layer silicates. M–O,OH bond lengths also were set within specified

https://doi.org/10.1346/CCMN.1983.0310203 Published online by Cambridge University Press

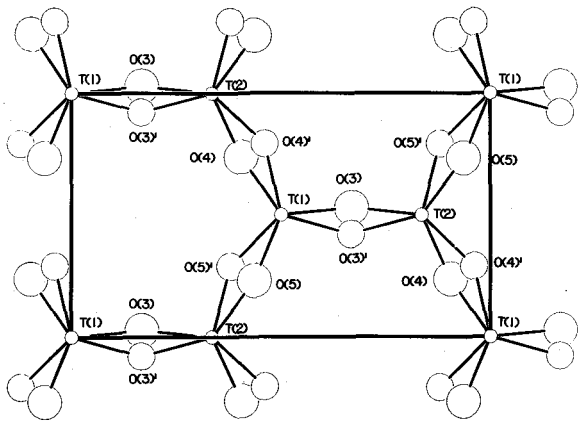


Figure 3. Projection onto (001) of the tetrahedral sheet in the first layer to illustrate the split basal oxygens.

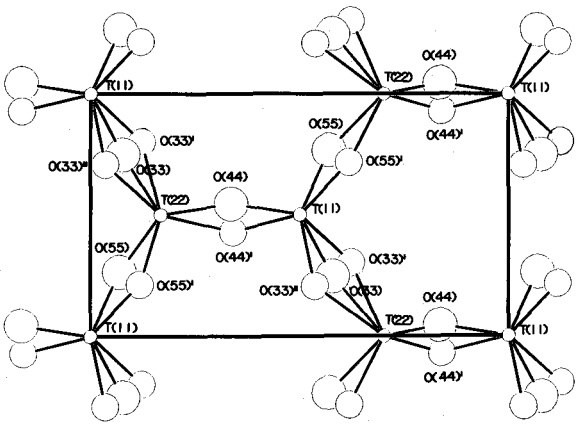


Figure 4. Projection onto (001) of the tetrahedral sheet in the second layer to illustrate the split basal oxygens.

limits. Multiplicities of all M sites, OH sites, apical oxygen sites, T(1), and T(11) were set equal to 1.0. Multiplicities of T(2), T(22), and all basal oxygens were set equal to 0.75. All extra "twin" positions [TwT(1), TwO(3), TwO(4), TwO(5), TwT(11), TwO(33), TwO(44), and TwO(55)] were set equal to 0.25. These last two sets of multiplicities then were varied so that their multiplicities remained equal within each group but supplementary between groups (x and 1 − x). Thermal parameters also were varied as rigid groups in the following manner: all M sites equal, all OH groups equal [except OH(1) and OH(11)], all basal oxygens equal, extra basal oxygens of the first layer equal, extra basal oxygens of the second layer equal, and split basal oxygens (O′ or O″) equal (see discussion of split basal oxygens below). All other thermal parameters were varied independently. Positions that retained reasonable isotropic thermal parameters were left unchanged; otherwise anisotropic refinement was attempted.

Throughout the late stages in the refinement, Fourier and Fourier-difference maps were constructed to modify or verify ordering patterns for all cation sites. Near the end of the refinement at (R ~6%) excess electron density was observed in the form of shadow peaks near each of the normal basal oxygens. These seven extra peaks could not be interpreted as a function of anisotropic thermal motion within the normal basal oxygens. Therefore, the positions of these split basal oxygens were added to the least squares refinement using coordinates taken from Fourier difference maps and designated O(3)′, O(4)′, O(5)′, O(33)′, O(33)″, O(44)′, and O(55)′. Figures 3 and 4 illustrate the split oxygen positions. Initial multiplicities of the split basal oxygens were assigned a value equal to 40% (0.4 × 0.8922 = 0.36) of the multiplicities of the normal basal oxygens. The remaining multiplicity (0.8922 − 0.36, or 60% of 0.8922) was reassigned to the normal basal oxygens. All multiplicities were varied as a rigid group. No attempt was made to locate hydrogen atoms in the late stages of refinement

The final residual factor R equaled 5.36%, with $R(F) = \Sigma\left|F_0 - F_c\right|/\Sigma F_0$. $R(F^2)$ equaled 8.59%, with $R(F^2) = \Sigma\left|F_0^2 - \left|F_c\right|^2\right|/\Sigma F_0^2$. The goodness-of-fit equaled 1.61 with $E\theta F = [\Sigma w(F_0 - F_c)^2/\text{N.O.} - \text{N.V.T.}]$. The final multiplicity for tetrahedra in the normal part of the structure was 0.89 and that for tetrahedra in the out-of-step domains was 0.11. The split basal oxygens had final multiplicities of 0.26 relative to 0.63 for the normal basal oxygens. The final atomic coordinates, isotropic thermal parameters, and bond lengths are reported in Tables 2 and 3. Tables of F_0, F_c, and anisotropic thermal parameters can be obtained from S. W. Bailey upon request.

DISCUSSION

Cation ordering

It is concluded on the basis of electron density and electron-density difference maps that Si and Fe^{3+} are ordered in tetrahedral positions. Fe^{3+} is strongly partitioned into T(1), T(11), TwT(1), and TwT(11), such that each of these sites contains approximately 50% Fe^{3+} and 50% Si. T(2), T(22), TwT(2), and TwT(22) consist entirely of Si. This determination takes into account the final multiplicities of 0.89 for tetraheda in the normal $2H_2$ portion of the structure and of 0.11 for those in the out-of-step domains. Mean tetrahedral bond lengths were not used as criteria for this determination (see below). It appears that tetrahedral ordering is complete, but small inconsistencies in the Fourier maps may indicate minor departures from total ordering. Tetrahedral ordering has no effect on lowering the symmetry from $P6_3$ to $P1$ (or $C1$ as oriented here), as the 6_3 screw axis that passes through the origin is parallel to Z and relates T(1) with T(11) and T(2) with T(22). Assuming that both T(1) and T(11) have identical Fe^{3+} concentrations, no reduction in symmetry would result from the

https://doi.org/10.1346/CCMN.1983.0310203 Published online by Cambridge University Press

Table 2. Final atomic coordinates.

No.	Atom	x	y	z	B_{equiv}
1	T1	0.0000(0)	0.0000(0)	0.0410(0)	1.34
2	T2	0.0005(7)	0.3349(4)	0.0362(3)	0.84
3	M1	0.1674(5)	0.1667(3)	0.2372(2)	0.92
4	M2	0.6688(5)	0.0001(3)	0.2372(2)	0.92
5	M3	0.6682(5)	0.3340(3)	0.2371(2)	0.92
6	O1	0.0015(11)	0.0003(5)	0.1587(6)	1.49
7	O2	0.0013(11)	0.3338(5)	0.1594(6)	1.49
8	O3	−0.0287(27)	0.1677(9)	0.0042(9)	3.15
9	O4	0.2623(19)	0.4054(14)	0.0011(8)	3.15
10	O5	0.2684(19)	−0.0636(14)	0.0027(8)	3.15
11	OH1	0.5017(9)	0.1672(7)	0.1601(6)	1.44
12	OH2	0.3357(8)	0.0006(4)	0.3070(4)	1.27
13	OH3	0.3350(7)	0.3331(4)	0.3070(4)	1.27
14	OH4	0.8345(7)	0.1673(4)	0.3070(4)	1.27
15	T11	−0.0006(3)	0.0001(2)	0.5406(2)	1.06
16	T22	0.4997(9)	0.1678(5)	0.5356(4)	1.35
17	M11	0.3355(5)	0.3339(3)	0.7373(2)	0.92
18	M22	0.3338(5)	0.0004(2)	0.7372(2)	0.92
19	M33	0.8347(5)	0.1665(3)	0.7372(2)	0.92
20	O11	0.0016(7)	0.0000(4)	0.6595(6)	1.64
21	O22	0.5011(7)	0.1671(4)	0.6602(5)	1.64
22	O33	0.2519(21)	0.0786(15)	0.5039(9)	3.15
23	O44	0.4541(27)	0.3352(10)	0.5061(8)	3.15
24	O55	−0.2654(22)	0.0699(15)	0.5017(9)	3.15
25	OH11	0.0021(7)	0.3336(4)	0.6608(6)	1.49
26	OH22	0.6677(7)	0.3332(4)	0.8079(4)	1.27
27	OH33	0.6673(7)	−0.0003(4)	0.8078(4)	1.27
28	OH44	0.1685(8)	0.1679(4)	0.8077(4)	1.27
29	TwT1	0.0333(−)	0.6627(−)	0.0410(−)	1.27
30	TwO3	0.5398(−)	0.3189(−)	−0.0029(−)	1.22
31	TwO4	0.2485(−)	0.1238(−)	0.0595(−)	1.22
32	TwO5	0.7617(−)	0.0743(−)	0.0768(−)	1.22
33	TwT11	0.0174(−)	0.3269(−)	0.5432(−)	0.32
34	TwO33	0.2540(−)	0.8790(−)	0.5011(−)	2.12
35	TwO44	0.4622(−)	0.6638(−)	0.5057(−)	2.12
36	TwO55	0.7304(−)	0.9262(−)	0.4941(−)	2.12
37	O5′	0.2097(43)	−0.1206(28)	0.0019(19)	2.28
38	O3′	0.0787(52)	0.1668(18)	0.0047(20)	2.28
39	O4′	−0.2908(36)	−0.0388(31)	0.0037(20)	2.28
40	O33′	0.1966(45)	0.1231(26)	0.4985(20)	2.28
41	O33″	0.2915(32)	0.0363(29)	0.5091(21)	2.28
42	O44′	0.0697(53)	−0.1640(20)	0.5006(19)	2.28
43	O55′	−0.2153(42)	0.1187(25)	0.5062(21)	2.28

ordering itself. From Figures 1 and 2, however, it is evident that the ordering pattern observed in the normal $2H_2$ part of the structure is reversed in the out-of-step domains.

In contrast to the tetrahedral cations, the octahedral cations are disordered over all M sites. Mean M–O,OH bonds for all sites have similar lengths (2.102 to 2.107 Å), indicating no substantial ordering of Fe^{2+}, Fe^{3+}, Mg, or Mn, and are in good agreement with the bond length of 2.100 Å calculated from the electron-probe composition and the effective ionic radii of Shannon (1976). Final electron-difference maps showed no peaks in excess of one electron. So, unlike amesite-$2H_2$, cronstedtite-$2H_2$ has no localization of the charge balance between the tetrahedral and octahedral sheets as a result of the ordering pattern. Instead, the major M cations are distributed randomly and an electron-hopping effect between Fe^{2+} and Fe^{3+} probably is present.

Tetrahedral bond lengths

Mean tetrahedral bond lengths in the normal $2H_2$ portion of the structure do not verify the ordering pattern given by the electron distributions. Mean T–O bond lengths (Table 3) for T(1) and T(2) are identical (1.68 Å), although slightly greater for T(22) (1.69 Å) compared to T(11) (1.67 Å). Bond lengths are not listed in Table 3 for the out-of-step domains because they were determined with less accuracy. The mean T–O bond lengths in the latter domains are 1.63 Å for TwT(1) and 1.66 Å for TwT(11). The evidence from the T–O bond lengths is contradictory to that of the electron density and, if considered by itself, indicates tetrahedral cation

https://doi.org/10.1346/CCMN.1983.0310203 Published online by Cambridge University Press

Table 3. Calculated bond lengths (Å) and angles (°).

Tetrahedron T(1)

O(1)	1.676(8)	O(1)–O(3)	2.717(13)	O(1)–O(3)	108.11(46)
O(3)	1.679(9)	–O(4)	2.749(12)	–O(4)	110.06(calc)
O(4)	1.678(8)	–O(5)	2.726(13)	–O(5)	108.73(47)
O(5)	1.678(9)	O(3)–O(4)	2.754(17)	O(3)–O(4)	110.36(calc)
mean	1.678	–O(5)	2.727(17)	–O(5)	108.64(64)
		O(4)–O(5)	2.719(17)	O(4)–O(5)	112.17(calc)
		mean	2.732	mean	109.68

Tetrahedron T(2)

O(2)	1.754(9)	O(2)–O(3)	2.717(13)	O(2)–O(3)	105.64(46)
O(3)	1.655(9)	–O(4)	2.753(12)	–O(4)	107.55(45)
O(4)	1.658(8)	–O(5)	2.747(12)	–O(5)	107.01(44)
O(5)	1.662(9)	O(3)–O(4)	2.735(17)	O(3)–O(4)	112.65(67)
mean	1.682	–O(5)	2.775(17)	–O(5)	113.58(64)
		O(4)–O(5)	2.785(17)	O(4)–O(5)	109.97(66)
		mean	2.752	mean	109.40

T(1)–O(3)–T(2)	144.05(76)	O(4)–O(5)–O(3)	132.79(73)
T(1)–O(4)–T(2)	141.51(69)		108.45(calc)
T(1)–O(5)–T(2)	141.51(73)	O(5)–O(3)–O(4)	108.11(71)
O(3)–O(4)–O(5)	131.33(72)		135.87(calc)
	108.51(35)		

Tetrahedron T(11)

O(11)	1.694(8)	O(11)–O(33)	2.709(13)	O(11)–O(33)	108.06(49)
O(33)	1.653(10)	–O(44)	2.697(13)	–O(44)	105.86(calc)
O(44)	1.686(11)	–O(55)	2.761(14)	–O(55)	109.51(45)
O(55)	1.658(9)	O(33)–O(44)	2.822(18)	O(33)–O(44)	115.38(calc)
mean	1.673	–O(55)	2.643(18)	–O(55)	116.01(68)
		O(44)–O(55)	2.527(18)	O(44)–O(55)	98.17(calc)
		mean	2.693	mean	108.83

Tetrahedron T(22)

O(22)	1.776(8)	O(22)–O(33)	2.742(14)	O(22)–O(33)	105.85(49)
O(33)	1.660(10)	–O(44)	2.723(12)	–O(44)	104.89(46)
O(44)	1.658(9)	–O(55)	2.752(13)	–O(55)	106.59(48)
O(55)	1.656(9)	O(33)–O(44)	2.669(18)	O(33)–O(44)	107.14(66)
mean	1.688	–O(55)	2.832(18)	–O(55)	105.68(69)
		O(44)–O(55)	2.943(18)	O(44)–O(55)	125.32(66)
		mean	2.777	mean	109.25

T(11)–O(33)–T(22)	145.64(87)	O(33)–O(55)–O(44)	119.77(69)
T(11)–O(44)–T(22)	143.52(75)		124.25(calc)
T(11)–O(55)–T(22)	142.29(82)	O(44)–O(33)–O(55)	116.13(72)
O(33)–O(44)–O(55)	127.09(80)		120.37(calc)
	113.26(71)		

Octahedron

	M(1)	M(2)	M(3)
O(1)–O(2)	3.157(6)	3.158(7)	3.157(7)
–OH(1)	3.161(7)	3.159(7)	3.153(6)
O(2)–OH(1)	3.160(6)	3.156(6)	3.156(6)
OH(2)–OH(3)	3.148(5)	3.159(5)	3.165(5)
–OH(4)	3.164(6)	3.153(5)	3.155(5)
OH(3)–OH(4)	3.157(5)	3.163(5)	3.152(5)
mean unshared	3.158	3.158	3.156
O(1)–OH(2)	2.793(8)	—	2.793(8)
–OH(3)	—	2.791(8)	2.791(8)
–OH(4)	2.791(8)	2.791(8)	—
O(2)–OH(2)	—	2.780(8)	2.780(8)
–OH(3)	2.784(8)	2.784(8)	—
–OH(4)	2.781(8)	—	2.781(8)
OH(1)–OH(2)	2.773(8)	2.773(8)	—
–OH(3)	2.770(8)	—	2.770(8)
–OH(4)	—	2.773(8)	2.773(8)
mean shared	2.782	2.782	2.781

https://doi.org/10.1346/CCMN.1983.0310203 Published online by Cambridge University Press

Table 3. Continued.

	M(11)	M(22)	M(33)
O(11)–O(22)	3.152(5)	3.158(5)	3.163(5)
–OH(11)	3.155(5)	3.159(5)	3.158(5)
O(22)–OH(11)	3.153(5)	3.157(5)	3.162(5)
OH(22)–OH(33)	3.156(5)	3.159(5)	3.157(5)
–OH(44)	3.148(5)	3.168(5)	3.156(5)
OH(33)–OH(44)	3.141(5)	3.160(5)	3.171(5)
mean unshared	3.151	3.160	3.161
O(11)–OH(22)	2.790(7)	2.790(7)	—
–OH(33)	2.793(7)	—	2.793(7)
–OH(44)	—	2.795(7)	2.795(7)
O(22)–OH(22)	2.779(7)	—	2.779(7)
–OH(33)	—	2.784(7)	2.784(7)
–OH(44)	2.779(7)	2.779(7)	—
OH(11)–OH(22)	—	2.782(7)	2.782(7)
–OH(33)	2.770(7)	2.770(7)	—
–OH(44)	2.770(7)	—	2.770(7)
mean shared	2.780	2.783	2.784

Octahedron M(1)		Octahedron M(11)	
O(1)–O(2)	95.39(28)	O(11)–O(22)	95.64(23)
–OH(1)	95.54(28)	–OH(11)	95.80(24)
O(2)–OH(1)	95.53(28)	O(22)–OH(11)	95.76(23)
OH(2)–OH(3)	98.63(19)	OH(22)–OH(33)	98.99(19)
–OH(4)	99.33(19)	–OH(44)	98.55(19)
OH(3)–OH(4)	99.04(19)	OH(33)–OH(44)	98.24(19)
mean	97.24	mean	97.16
Octahedron M(2)		**Octahedron M(22)**	
O(1)–O(2)	95.48(26)	O(11)–O(22)	95.81(23)
–OH(1)	95.50(26)	–OH(11)	95.89(24)
O(2)–OH(1)	95.52(26)	O(22)–OH(11)	95.78(23)
OH(2)–OH(3)	99.02(19)	OH(22)–OH(33)	98.56(calc)
–OH(4)	98.76(19)	–OH(44)	98.94(calc)
OH(3)–OH(4)	99.18(19)	OH(33)–OH(44)	98.64(19)
mean	97.24	mean	97.27
Octahedron M(3)		**Octahedron M(33)**	
O(1)–O(2)	95.42(26)	O(11)–O(22)	95.87(24)
–OH(1)	95.42(26)	–OH(11)	95.72(24)
O(2)–OH(1)	95.61(26)	O(22)–OH(11)	95.94(23)
OH(2)–OH(3)	99.28(19)	OH(22)–OH(33)	98.53(19)
–OH(4)	98.88(19)	–OH(44)	98.44(19)
OH(3)–OH(4)	98.76(19)	OH(33)–OH(44)	99.09(19)
mean	97.23	mean	97.27
Interlayer contact			
OH(2)–O(33)	2.936(14)	OH(22)–O(5)	2.992
OH(3)–O(44)	2.910(13)	OH(33)–O(4)	2.940
OH(4)–O(55)	2.973(14)	OH(44)–O(3)	3.000

disorder. As mentioned above Fe^{3+} (high spin) and Si^{4+} have drastically different ionic radii, and hence their corresponding tetrahedral bond lengths should be quite different (calculated values of 1.85 Å and 1.62 Å, respectively). Because the electron density must be considered definitive as to the ordering pattern, the following mean T–O bond lengths are expected: T(1) = T(11) = 1.73 Å and T(2) = T(22) = 1.62 Å. This was not observed. Assuming that the data are correct (and there is no reason *a priori* why they should not be, as X-ray diffraction films display near-perfect Bragg reflections and the final R factor is quite good), some mechanism(s) must account for this discrepancy in bond lengths relative to electron densities.

The observed T(2)–O(2) (1.754 Å) and T(22)–O(22) (1.776 Å) apical bonds in the Si-rich tetrahedra are extremely elongate. Elongation of tetrahedra is observed in many layer silicates, but not to this extent. Mean $T–O_b$ lengths for T(2) and T(22) are both 1.658 Å. These lengths are greater by 0.04 Å than calculated values based on the assigned cation occupancies. Mean T(1)–O (1.678 Å) and T(11)–O (1.673 Å) bond lengths

https://doi.org/10.1346/CCMN.1983.0310203 Published online by Cambridge University Press

are even more difficult to explain. The Fe-rich tetrahedra indicate considerable contraction and electronic overlap based on published ionic radii (Shannon, 1976), whereas the Si-rich tetrahedra are overly large. Nevertheless, the grand mean of all T–O bonds of 1.680 Å is in good agreement with the value of 1.675 Å expected from the bulk tetrahedral composition and standard radii.

Previous X-ray diffraction studies of 1*M* Fe-rich micas have shown that tetrahedral cation assignments can be made for Fe^{3+} and Si based on observed mean bond lengths, at least in the disordered state (Donnay *et al.*, 1964; Steinfink, 1962). In each of these studies electron density maps were calculated using the ideal space group *C*2/*m* for the 1*M* mica polytype. This symmetry requires disorder of tetrahedral cations so that no discrepancy between electron density and bond lengths is possible. The failure of the bond lengths to agree with the electron density in the present study may involve the following factors:

(1) The basal oxygens have large apparent thermal parameters (Table 2). This effect is not a result solely of thermal motion, but is also a function of positional disorder, and has been observed in many silicate minerals (Burnham, 1973). Comparison of anisotropic thermal vibration ellipsoids for oxygen atoms surrounding tetrahedral sites containing only Si vs. those containing a hybrid Si,Al atom (disordered), shows this effect quite well. In tetrahedra with disordered Si,Al the apparent displacement of oxygen toward the average cation is approximately 0.1 Å or more, twice that of an oxygen coordinated to an ordered site. This difference results from the difference in Si–O and Al–O bond lengths, ~0.15 Å. Hence, in cronstedtite, where T(1) = $Fe^{3+}_{0.5}Si_{0.5}$, there should be a very distinct positional disorder of the coordinating oxygens, thereby accounting in part for the large thermal parameters of the basal oxygens. Thermal parameters of apical oxygens are less than those of the basal oxygens, probably due to bonding of each apical oxygen to three octahedral cations in addition to its tetrahedral cation. This type of positional disorder of the basal oxygens in cronstedtite may have some effect on the anomalous T–O bond lengths, but cannot account alone for the gross differences between the observed and calculated values.

(2) In addition to the large apparent thermal parameters, the basal oxygens are split into two electron density maxima [three in the case of O(33)], with final multiplicities of 0.63 and 0.26 from least-squares refinement. The new maxima are in the wrong positions to be correlated with the extra tetrahedra of the out-of-step domains and must represent a third kind of domain in which the direction of tetrahedral rotation is reversed (Figures 3, 4). The maxima of the extra basal oxygens [TwO(3–5) and TwO(33–55)] in the out-of-step domains are too weak to be able to tell if these are split in a similar fashion. The splitting of basal oxygens is another reason why the least squares minimization of atomic positions may be somewhat inaccurate, but any errors are believed to be insufficient to account for the large T–O bond discrepancies.

(3) Contraction of the Fe^{3+}–O bond length would be expected if an appreciable amount of π-bonding is present or if Fe^{3+} is present in low-spin instead of high-spin configuration. Sufficient material was not available to test for these possibilities, but they are unlikely solutions because they would not explain the equally anomalous Si–O bond lengths.

(4) In an attempt to maintain a semiregular tetrahedral sheet, it is possible that the large Fe tetrahedra contract and the smaller Si tetrahedra expand to allow a more regular and less distorted structure. Inasmuch as no layer silicate structure having an ordered tetrahedral distribution of Si and Fe^{3+} has been described, this mechanism has never been proposed. It has been well established, though, that a variety of mechanisms exist for structural adjustment in layer silicates so that misfit between octahedral and tetrahedral sheets can be minimized (Bailey, 1966). The apical oxygens in each layer of this structure are essentially coplanar, differing in z height by only 0.01 Å. The Fe-rich hybrid atoms in sites T(1) and T(11) are 0.07 Å higher than the Si-rich T(2) and T(22) atoms. If the apical oxygens were at positions expected from their ionic radii, there would be a corrugation of the upper surface of the tetrahedral sheet amounting to 0.18 Å. A corrugation of this magnitude may not be compatible with stability, so that the apical oxygens adopt compromise positions. Similar reasoning can be applied to the basal oxygens. Proof of the validity of this argument must await the discovery of a second ordered tetrahedral Si,Fe^{3+} distribution where both the bond lengths and the electron density are examined critically. Evidence against the argument comes from (a) the failure of a distance-least-squares program OPTDIS to duplicate the observed atomic positions based on several reasonable bond-weighting schemes for an ordered tetrahedral distribution of Si and Fe^{3+}, and (b) recent structural determinations of silicate minerals that show Si–O bond lengths to be relatively inflexible even at high temperatures and pressures.

Domain structures

Figures 1 and 2 show the presence of a tetrahedral sheet in each layer that appears to be out-of-step by $b/3$ relative to the rest of the structure. This is due to a stacking mistake of zero shift interspersed with the nor-

https://doi.org/10.1346/CCMN.1983.0310203 Published online by Cambridge University Press

mal alternation of $-b/3$ and $+b/3$ shifts of the $2H_2$ polytype. There is no interruption of the regular alternation of occupation of the I and II sets of octahedral positions in adjacent layers (equivalent to 180° rotations). In these out-of-step domains the tetrahedral ordering pattern is reversed. Thus, Fe-rich site T(11) at the top of a slab of the normal $2H_2$ structure is succeeded by a Si-rich site TwT(2) in the out-of-step domain immediately above, instead of by the Fe-rich site T(1) of the normal structure, and Si-rich site T(22) is succeeded at the same time by the Fe-rich site TwT(1). The two layers forming the interface between the normal structure and the out-of-step domain constitute an ordered $2H_1$ sequence, whereas each out-of-step domain has a $2H_2$ sequence of layers at least 10 unit cells thick and enantiomorphic to that of the normal $2H_2$ structure (i.e., the interlayer shift between layers 1 and 2 is $+b/3$ instead of $-b/3$). It may be an important point in the origin of these domains that this reversal of the ordering pattern would serve to alleviate strains caused by tetrahedral ordering in adjacent parts of the crystal, so that strain relief may cause the stacking mistakes. The crystal fragment used contains about 11% of these out-of-step domains.

A different kind of domain gives rise to the split basal oxygen atoms illustrated in Figures 3 and 4. These are interpreted as regions in which the direction of tetrahedral rotation is reversed relative to that in the rest of the structure. The direction of rotation in 1:1 layer silicates is controlled by competition between attraction of the basal oxygens by (1) octahedral cations in the layer below, (2) octahedral cations in their own layer, and (3) OH groups on the layer surface immediately below (Bailey, 1966). In amesite-$2H_2$ factors (2) and (3) combine to overcome the attraction of cations in the layer below. In this crystal of cronstedtite-$2H_2$ about 74% of the volume contains tetrahedra rotated in the opposite sense, but similar to the direction found by Steadman and Nuttall (1963) for the $1T$ and $6R_2$ forms of cronstedtite, and 26% rotated in the same sense as in amesite-$2H_2$. The influence of directed interlayer H-bonds on the rotation direction in this cronstedtite crystal may be cancelled by octahedral cation disorder and electron hopping leading to H disorder. The difficulty in determining the centers of the split basal oxygens is emphasized by the irregularity of splitting and tetrahedral rotation in the second layer where O(33) is apparently split into three parts (for reasons not understood) and adjacent atoms O(44) and O(55) both rotate towards the ring center (Figure 4), which is a physical impossibility. For these reasons the 6.2° rotation angle in the first layer is considered the most reliable value.

More information on the nature of the domains may be contained in the possible non-Bragg satellites noticed on $hk0$ Weissenberg photographs of the large parent crystal. These have been ignored in the present study because they could not be observed with exposure times up to 70 hr on $hk0$ precession films of the smaller crystal.

Subgroup symmetry

The ideal space group for the $2H_2$ polytype is $P6_3$, but the diffraction intensities indicate $P1$ symmetry. This reduction to subgroup symmetry is not due to cation ordering, however, as the pattern of tetrahedral ordering does not violate $P6_3$ symmetry and the octahedral cations are disordered. The lower symmetry, therefore, must be due to a combination of the contributions of the three kinds of domains to the coincident reflections and of non-hexagonal distortions to the structure as a consequence of attempting to keep a regular tetrahedral sheet shape despite the ordering. Analysis of the positions of the basal oxygens relative to their errors of determination shows that they deviate in position from hexagonal symmetry by a minimum of 9.8 and a maximum of 23.3 standard deviations.

Other features

All six octahedra are nearly identical in size and shape due to the disordered cation distribution. The angle of octahedral flattening ψ is 60.05° relative to 54.73° for a regular octahedron. The octahedral distortion parameter defined by Dollase (1969) is rms = 5.6° and that of Robinson *et al.* (1971) is $(\sigma\theta)^2 = 58.8°$. The tetrahedra are severely distorted with τ values for Fe-rich T(1) and T(11) of 109.0 and 107.8° and for Si-rich T(2) and T(22) of 106.7 and 105.8. The sheet thicknesses are comparable to those of other Fe-rich trioctahedral layer silicates. The two tetrahedral sheet thicknesses are 2.232 and 2.225 Å, those of the octahedral sheets are 2.102 and 2.103 Å, and the interlayer spaces are 2.804 and 2.775 Å to give a total c repeat of 14.241 Å.

ACKNOWLEDGMENTS

The specimen used in this study was kindly donated by Professor J. J. Finney of the Colorado School of Mines. This research has been supported in part by the National Science Foundation, grants EAR78-05394 and EAR81-6124, and in part by the Petroleum Research Fund, grants 11224-AC2 and 13157-AC2-C, administered by the American Chemical Society. We appreciate the advice and the use of facilities of Professor L. F. Dahl of the Department of Chemistry, University of Wisconsin.

REFERENCES

Anderson, C. S. and Bailey, S. W. (1981) A new cation ordering pattern in amesite-$2H_2$: *Amer. Mineral.* **66,** 185–195.

Bailey, S. W. (1966) The status of clay mineral structures: in *Clays and Clay Minerals, Proc. 14th Natl. Conf., Berkeley, California, 1965,* S. W. Bailey, ed., Pergamon Press, New York, 1–23.

Bailey, S. W. (1969) Polymorphism of trioctahedral 1:1 layer silicates: *Clays & Clay Minerals* **17,** 355–371.

https://doi.org/10.1346/CCMN.1983.0310203 Published online by Cambridge University Press

Bailey, S. W. (1975) Cation ordering and pseudosymmetry in layer silicates: *Amer. Mineral.* **60,** 175–187.

Barber, D. J. (1981) Matrix phyllosilicates and associated minerals in C2M carbonaceous chondrites: *Geochim. Cosmochim. Acta* **45,** 945–970.

Burnham, C. W. (1973) Order-disorder relationships in some rock-forming silicate minerals: *Annu. Rev. Earth Planet. Sci.* **1,** 313–339.

Dollase, W. A. (1969) Crystal structure and cation ordering of piemontite: *Amer. Mineral.* **54,** 710–717.

Donnay, G., Morimoto, N., Takeda, H., and Donnay, J. D. H. (1964) Trioctahedral one-layer micas. I. Crystal structure of a synthetic iron mica: *Acta Crystallogr.* **17,** 1369–1373.

Frondel, C. (1962) Polytypism in cronstedtite: *Amer. Mineral.* **47,** 781–783.

Gole, M. J. (1980) Low-temperature retrograde minerals in metamorphosed Archean banded iron-formations, Western Australia: *Canadian Mineral.* **18,** 205–214.

Hall, S. H. and Bailey, S. W. (1979) Cation ordering pattern in amesite. *Clays & Clay Minerals* **27,** 241–247.

Henry, D. L. (1974) The crystal structure of cronstedtite-$2H_2$: M.S. Thesis, University of Wsiconsin–Madison, Wisconsin. 46 pp.

Müller, W. F., Kurat, G., and Kracher, A. (1979) Chemical and crystallographic study of cronstedtite in the matrix of the Cochabamba (CM2) carbonaceous chondrite: *Tshermaks Mineral. Petrogr. Mitt.* **26,** 293–304.

Pattiaratchi, D. B., Saari, E., and Sahama, Th. G. (1967) Anandite, a new barium iron silicate from Wilagedra, North Western Province, Ceylon: *Min. Mag.* **36,** 1–4.

Robinson, K., Gibbs, G. V., and Ribbe, P. H. (1971) Quadratic elongation: a quantitative measure of distortion in coordination polyhedra: *Science* **172,** 567–570.

Shannon, R. D. (1976) Revised effective ionic radii and systematic studies of interatomic distance in halides and chalcogenides: *Acta Crystallogr.* **A32,** 751–767.

Steadman, R. and Nuttall, P. M. (1963) Polymorphism in cronstedtite: *Acta Crystallogr.* **16,** 1–8.

Steadman, R. and Nuttall, P. M. (1964) Further polymorphism in cronstedtite: *Acta Crystallogr.* **17,** 404–406.

Steinfink, H. (1962) Crystal structure of a trioctahedral mica: phlogopite: *Amer. Mineral.* **47,** 886–896.

Weisz, O., Cochran, W., and Cole, W. F. (1948) The accurate determination of cell dimensions from single-crystal X-ray photographs: *Acta Crystallogr.* **1,** 83–88.

(Received 25 February 1982; accepted 6 June 1982)

Резюме—Кристаллическая структура магниевого кроншедтита-$2H_2$ из Прибрам, Чехословакия была усовершенствована в пространственной группе C1 при помощи 1832 независимых отражений так, что указатель различия составлял 5,4%. Тетраэдрическое упорядочение между Fe^{3+} и Si кажется быть полным на основе карт плотности электронов, что является первым подтверждением такого упорядочения в слоистом силикате. Октаэдрические катионы являются неупорядоченными на местах M. Средние длины связи T–O не подтверждают тетраэдрическое упорядочение, возможно, вследствие тетраэдрического отклонения, необходимого для освобождения экстремальной волнистости слоя, которая появилась бы в результате упорядочения катионов так разных размеров.

В начальных стадиях усовершенствования структура исследуемого кристалла не могла быть адекватно описана на основе единичного политипа $2H_2$. Структура содержит два типа областей $2H_2$, которые казались быть сдвинутыми о $b/3$ по отношению одна к другой вследствие ошибки в последовательности чередования слоев. Ошибка нулевого сдвига (обыкновенный политип $2H_2$ состоит из изменяющихся сдвигов $-b/3$ и $+b/3$) влияет только на тетраэдрические пластинки. Это создает прилегающие энантиоморфные области пакетов $2H_2$ такие, что области с малыми Si тетраэддами расположены над большими Fe^{3+} обогаченными тетраэдрами и наоборот. Этот механизм снятия напряжения может действительно быть причиной ошибок в чередовании. Третий тип области содержит зоны с обратной тетраэдрической ротацией, что вызывает появление раздвоенных основных атомов кислорода на картах плотности электронов. Эта модель многочисленных областей наилучшим образом объясняет дополнительные атомные места, наблюдаемые на картах Фурьера, недостаток отражений $k \neq 3n$ и возможные несущественные "сопутствующие" отражения, наблюдаемые ра фильмах Вейссенберга. [E.C.]

Resümee—Die Kristallstruktur von einem Mg-Kronstedtit-$2H_2$ von Příbram, Tschechoslowakei, wurde in der Raumgruppe $C1$ auf einen R-Wert von 5,4% bei 1832 unabhängigen Reflexen verfeinert. Aufgrund der Elektronendichteverteilung scheint die regelmäßige Tetraederverteilung zwischen Fe^{3+} und Si vollständig zu sein. Dies ist die erste Bestätigung für eine derartige Anordnung in einem Schichtsilikat. Die Oktaeder-Kationen sind auf den M-Plätzen statistisch verteilt. Die durchschnittlichen T–O-Bindungsabstände bestätigen die tetraedrische Anordnung nicht. Der Grund liegt vielleicht in einer Verzerrung der Tetraeder, wodurch die extreme Wellung der Schichten verringert wird, die durch die regelmäßige Verteilung von derartig unterschiedlichen großen Kationen verursacht wird.

Am Anfang des Verfeinerungsprozesses konnte die Struktur des untersuchten Kristalls nicht auf der Basis eines einzigen $2H_2$-Polytypen adäquat beschrieben werden. Die Struktur enthält zwei Arten von $2H_2$-Domänen, die um $b/3$ relativ zueinander verschoben zu sein scheinen, was auf einen Fehlbau in der Stapelabfolge zurückzuführen ist. Der Fehlbau der Null-Verschiebung (der normale $2H_2$-Polytyp besteht aus abwechselnden $-b/3$ und $+b/3$-Verschiebungen) beeinflußt nur die Tetraederschichten. Er verursacht benachbarte enantiomorphe Domänen von $2H_2$-Paketen in der Weise, daß Domänen mit kleinen Si-Tetraedern über größeren Fe^{3+}-reichen Tetraedern liegen und umgekehrt. Dieser Mechanismus zur Deformationsverminderung könnte tatsächlich die Ursache für die Stapelfehler sein. Eine dritte Art von Domänen enthält Bereiche, in denen die Richtung der Tetraederrotation umgedreht ist, wodurch die basalen Sauerstoffreflexe auf den Elektronendichteverteilungen aufgespalten sind. Dieses vielfältige Domänenmodell erklärt am besten besondere Atomlagen, die durch Fourieranalyse beobachtet wurden, das Fehlen von Streifen bei den $k \neq 3n$-Reflexen und mögliche nichtintegrale "Satelit"-Reflexe auf den Weißenbergfilmen. [U.W.]

https://doi.org/10.1346/CCMN.1983.0310203 Published online by Cambridge University Press

Résumé—La structure cristalline d'une cronstedtite-$2H_2$ de magnésium de Příbram, Tchéchoslovaquie, a été raffinée dans le groupe spatial $C1$ à un résidu de 5,4% avec 1832 réflections indépendantes. L'ordre tetraèdral entre Fe^{3+} et Si est jugé être complet basé sur des cartes de densité d'électrons, la première confirmation d'un tel ordre residant dans une couche silicate. Des cations octaèdraux sont désordonnés sur les sites M. Les longueurs de liaison T–O moyennes ne confirment pas l'ordre tetraèdral, peut-être à cause de la distortion tetraèdrale afin d'amoindrir l'extrême corrugation de la feuille à laquelle donnerait lieu l'ordre de cations de tailles tellement différentes.

Dans les stages initiales de l'étude, le cristal étudié ne pouvait être décrit de façon adéquate sur la base d'un seul polytype $2H_2$. La structure contient deux sortes de domaines $2H_2$ qui semblent déplacés de $b/3$ l'un par rapport à l'autre à cause d'une erreur dans la séquence d'emplilement intercouche. Cette erreur de déplacement zero (le polytype $2H_2$ normal consiste en des déplacements alternants $-b/3$ et $+b/3$) n'affecte que les feuilles tetraèdrales. Elle crée des domaines adjacents énantiomorphes de paquets $2H_2$ de telle façon que les domaines avec de petits tetraèdres Si se trouvent au dessus de tetraèdres riches en Fe^{3+} plus grands et vice-versa. Ce mécanisme pour soulager la tension peut en effet être la cause des erreurs d'empilement. Une troisième sorte de domaine contient des régions dans lesquelles le sens de la rotation est renversé, donnant lieu à des oxygènes de base fendus sur des cartes de densité d'électrons. Ce modèle de domaines multiples explique de la meilleure façon les positions atomiques supplémentaires observées sur les cartes Fourier, le manque de striations de réflections $k \neq 3n$ et des réflections nonintégrales "satellitiques" possibles observées sur les films Weissenberg. [D.J.]

https://doi.org/10.1346/CCMN.1983.0310203 Published online by Cambridge University Press